

INTERNATIONAL JOURNAL OF CHEMICAL REACTOR ENGINEERING

Volume 6

2008

Article A23

Dynamic Behaviour of a Continuous Heat Exchanger/Reactor after Flow Failure

Wassila Benaissa*

Sebastien Elgue[†]

Nadine Gabas[‡]

Michel Cabassud**

Douglas Carson^{††}

Michel Demissy^{‡‡}

*INERIS, joyfulwass@hotmail.com

[†]Ecole Nationale Supérieure des Ingénieurs en Arts Chimiques Et Technologiques, sebastien.elgue@ensiacet.fr

[‡]Ecole Nationale Supérieure des Ingénieurs en Arts Chimiques Et Technologiques, nadine.gabas@ensiacet.fr

**Laboratoire de Génie Chimique de Toulouse - UMR 5503 CNRS/INPT/UPS, michel.cabassud@ensiacet.fr

^{††}INERIS, douglas.carson@ineris.fr

^{‡‡}INERIS, michel.demissy@ineris.fr

ISSN 1542-6580

Copyright ©2008 The Berkeley Electronic Press. All rights reserved.

Dynamic Behaviour of a Continuous Heat Exchanger/Reactor after Flow Failure

Wassila Benaissa, Sebastien Elgue, Nadine Gabas, Michel Cabassud, Douglas Carson, and Michel Demissy

Abstract

The intensified technologies offer new prospects for the development of hazardous chemical syntheses in safer conditions: the idea is to reduce the reaction volume by increasing the thermal performances and preferring the continuous mode to the batch one. In particular, the Open Plate Reactor (OPR) type “reactor/exchanger” also including a modular block structure, matches these characteristics perfectly. The aim of this paper is to study the OPR behaviour during a normal operation, that is to say, after a stoppage of the circulation of the cooling fluid. So, an experiment was carried out, taking the oxidation of sodium thiosulfate with hydrogen peroxide as an example. The results obtained, in particular with regard to the evolution of the temperature profiles of the reaction medium as a function of time along the apparatus, are compared with those predicted by a dynamic simulator of the OPR. So, the average heat transfer coefficient regarding the “utility” fluid is evaluated in conductive and natural convection modes, and then integrated in the simulator. The conclusion of this study is that, during a cooling failure, a heat transfer by natural convection would be added to the conduction, which contributes to the intrinsically safer character of the apparatus.

KEYWORDS: heat exchanger/reactor, dynamic simulation, safety, failure mode, oxidation

1. INTRODUCTION

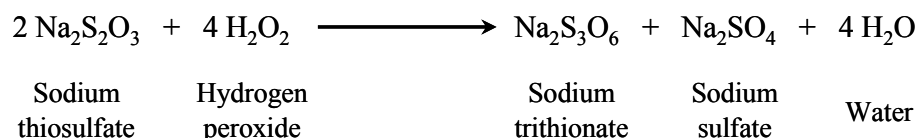
The principal tool for the development of hazardous chemical syntheses in the field of fine chemicals and pharmaceuticals remains the batch reactor. However, even if it offers the required flexibility and versatility, this type of reactor presents a number of technological limitations. In particular, poor heat transfer of the heat generated by exothermic chemical reactions is a serious problem with regard to safety (Stoessel, 1993). An alternative approach is presented by the recent evolution of micro/mini technologies. The idea is to transpose the reactions to plug flow reactors with intensification of the chemical synthesis process. The first benefit comes from a better control of heat exchange which makes it possible, on the one hand, to concentrate the reactants and thus limit the amount of solvent to be treated, and, on the other hand, to mix the reactants in an optimal way so as to obtain a better performance and a higher selectivity. Moreover, this kind of production makes it possible to manufacture the reaction products on-line, which limits storage and avoids using large capacities. During the last decades, a few devices with these characteristics have appeared. Because of their innovating features, bringing into service these reactors requires developing specific tools in the fields of control, simulation and safety, too. As a matter of fact, even if these new technologies are intrinsically safer due to their design, studies are necessary to estimate this assumption.

This article deals with the Open Plate Reactor (OPR) which is a continuous intensified “heat-exchanger/reactor” made up of a modular block structure. Several studies already dealt with the OPR performances through the implementation of several chemical reactions (Benaïssa et al., 2006; Benaïssa et al., 2005; Benaïssa, 2006; Prat et al., 2005). Moreover, in the parallel to the development of the OPR, a specific computer simulation program has been written. In this program, a complex dynamic model, integrating modelling of hydrodynamic, thermal and reaction aspects, allows one to reproduce and predict the reactor behaviour during normal operation. The program has already been tested on many experimental studies carried out during normal operation (Elgue et al., 2005).

In the field of safety, the aim of this work is now to study the behaviour of the OPR in a failure mode, that is after a failure in the circulation of the cooling fluid. In this respect, one experiment was carried out by stopping the cooling fluid when a fast, highly exothermic reaction was carried out in the OPR: the oxidation of sodium thiosulfate with hydrogen peroxide. The objective is to identify the thermal behaviour of the device and compare it to the predictions of the dynamic simulator with experimental data in order to check if the simulation tool, developed for normal operation, can be used to reproduce the failure mode.

2. CASE STUDY: OXIDATION OF SODIUM THIOSULFATE WITH HYDROGEN PEROXIDE

The oxidation of sodium thiosulfate with hydrogen peroxide leads to the formation of trithionate and sulfate, according to the following reaction scheme:



This reaction is generally operated in a homogeneous liquid medium and in batch mode. The operating temperature does not usually exceed 40°C. It is irreversible, very fast and strongly exothermic. The reaction enthalpy is - 586.2 kJ.mol⁻¹ of Na₂S₂O₃ (Lo et al., 1972). It can create safety problems related to the evacuation of heat released by the reaction. It is thus particularly interesting because it constitutes a fast reaction system that may be operated in a continuous reactor presenting short residence time. On the other hand, its highly energetic character makes it a case study particularly adapted to safety studies. Moreover, it was the subject of calorimetric (Lin et al., 1981) and kinetic (Cohen et al., 1962) measurements.

3. “HEAT-EXCHANGER/REACTOR” OPR

3.1 Experimental device

The OPR “heat-exchanger/reactor” was developed by Alfa Laval Vicarb company. This device is designed according to a plate exchanger type modular structure as shown in Figure 1. Each block is made of a 60 cm x 30 cm x 1.5 cm PEEK (polyetheretherketone) plate (RP), allowing the flow of the reaction medium (also called “process” fluid) located between two stainless steel plates containing the utility fluid (UF). Sandwich stainless steel plates (SP₁ and SP₂) are situated on each side of RP and UF. Furthermore, transition plates (TP) allow the thermal isolation of each block. The reactants are mixed in the inlet of the RP plate. This innovating “heat-exchanger/reactor” technique allows one to obtain a large exchange surface and a better control of heat exchanges.

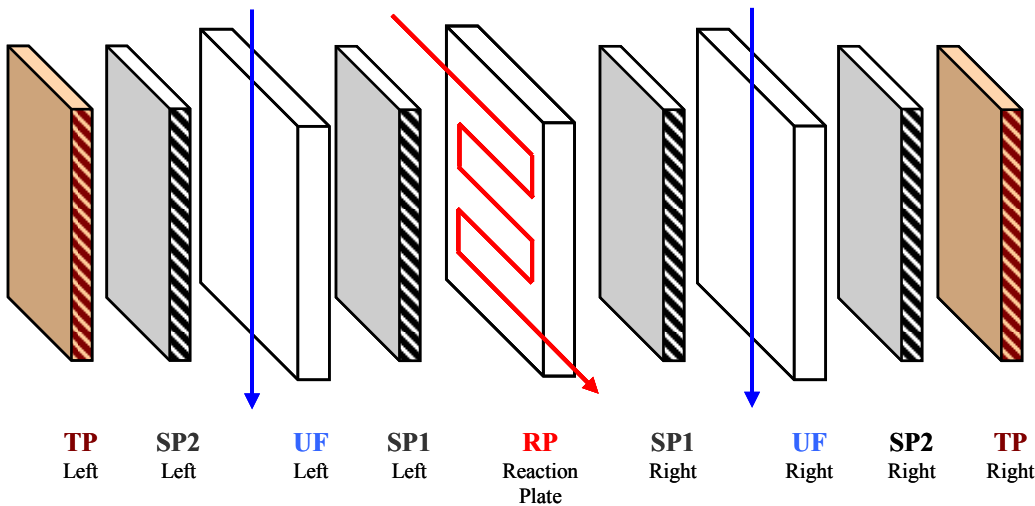


Figure 1. Successive plates contained in a block of the “heat-exchanger/reactor” OPR

The OPR pilot includes three blocks with a total capacity of 1.5 L. Preliminary hydrodynamic studies showed that for a total reactant flowrate of about 50 L.h⁻¹, the reactor has a perfectly plug flow behaviour. The OPR pilot used for the experiments was drilled in several spots, in order to introduce thermocouples inside the first RP plate to be able to follow the temperature evolution in the reaction line. Indeed, previous studies showed that most of the heat generated by the reaction was released in the first plate.

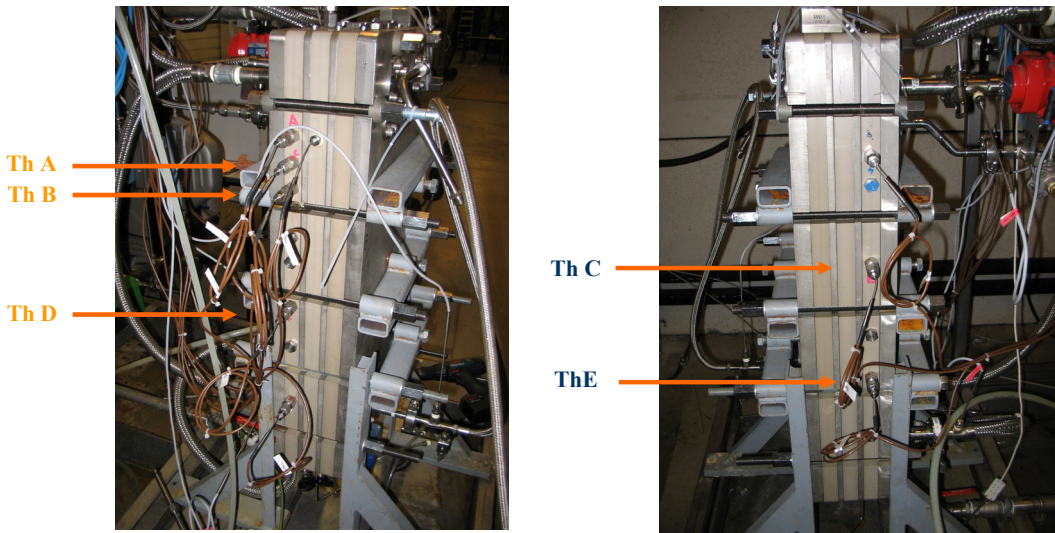


Figure 2. View of the two sides of the OPR and location of the thermocouples A to E

Figure 2 gives a view of the location of the thermocouples used in this study and appointed by the letters A to E. Table 1 gives for each thermocouple the volume covered by the reaction mixture from the inlet of the OPR.

Table 1. Reaction volume covered by the reaction mixture from the inlet of the OPR to the thermocouples

Thermocouples	Reaction volume (L)
Th A	0.0528
Th B	0.0859
Th C	0.1686
Th D	0.2513
Th E	0.3340
Total	1.5

3.2 Simulation tool

3.2.1 General structure of the model

A dynamic simulation tool of the OPR has been developed in order to predict the “heat-exchanger/reactor” behaviour according to the operating conditions (Elgue et al., 2005; Elgue et al., 2004). It integrates a precise description of the OPR geometry and models the hydrodynamic reaction phenomena as well as heat transfer in the device, which makes it possible to take into account the thermal inertia generated by the different plates previously described.

When normally operated, the flow and heat exchange modelling implies spatial cutting of the channels in which the “process” and “utility” fluids circulate, in modelled cells. The OPR is a continuous reactor with heat transfer taking place in the plates. Process flow modelling is therefore based on the classical representation of a sequence of perfectly stirred tank reactors (Neuman, 2002). Each model cell is assumed to be a perfectly stirred tank reactor. In this configuration, as shown in Figure 3, the entrance of a cell corresponds to the outlet of the previous one. The principal parameters are:

- Tp^k : temperature of the process fluid in the cell number k,
- Pp^k : pressure of the process fluid in the cell number k,
- Fp^k : flowrate of the process fluid in the cell number k,
- Xp^k : molar conversion of the process fluid in the cell number k,
- Tu_R^k : temperature of the utility fluid located on the right next to the cell number k,

- Fu_R^k : flowrate of the utility fluid located on the right next to the cell number k,
- Tu_L^k : temperature of the utility fluid located on the left next to the cell number k,
- Fu_R^k : flowrate of the utility fluid located on the left next to the cell number k.

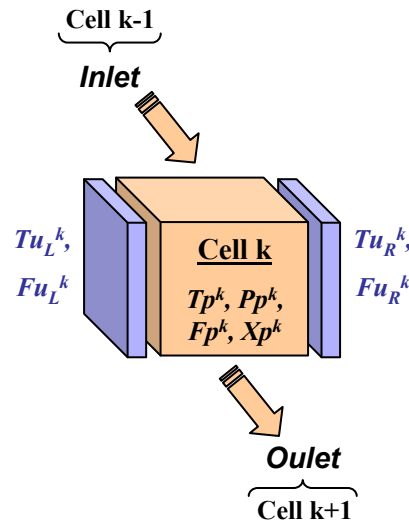


Figure 3. Description of an OPR modelling cell

In the case of a pilot plant composed of three blocks, experimental distribution of residence times, which allows flow analysis, showed that the reaction line could be described by a series of 91 cells which corresponds to the actual number of rows (see Figure 4).

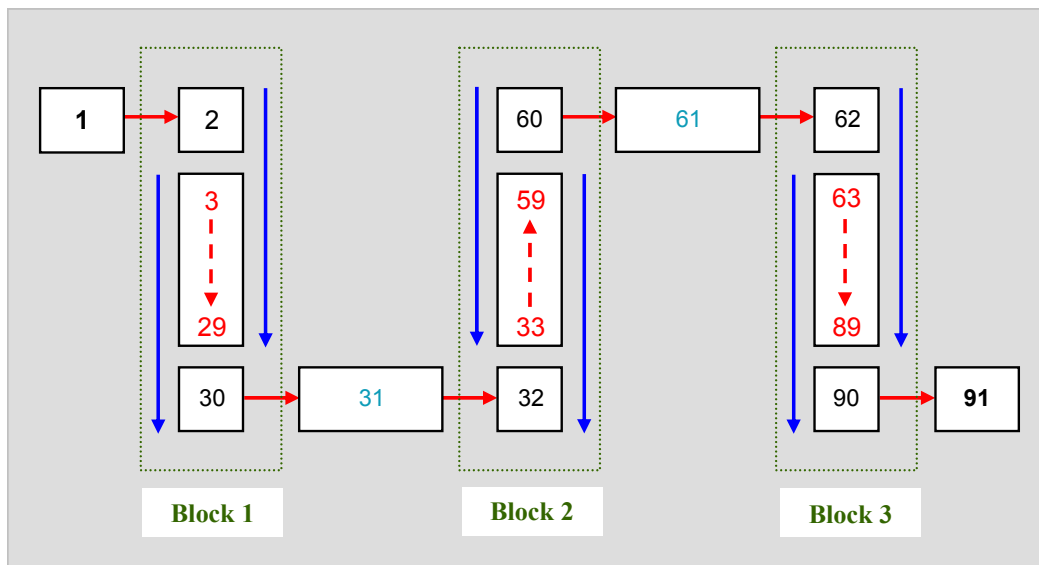


Figure 4. Reaction line modelling by a series of 91 stirred tank reactors (cells)

The modelling of a cell is then based on the expression of balances (mass and energy) and on constraint equations for each cell. The constraint equations are used to take into account the geometrical characteristics of the reactor and the physical properties of the medium considered. The balances may be used to describe the evolution of the characteristic values: temperature, composition, pressure according to the following dynamic formulation:

$$\{ Inlet \} + \{ Production \ flow \} = \{ Outlet \} + \{ Accumulation \ flow \}$$

Given the specific geometry of the reactor, two main parts may be distinguished. The first part is associated with the process plate where complex phenomena coupled with reaction and heat transfer take place. The second part encompasses the rest of the reactor structure, involving only heat transfer aspects.

3.2.2 Modelling of the process plate

The cells representing the process fluid circulating in the reaction plate are presumed to be filled with a perfectly stirred homogeneous medium which presents the following characteristics:

- Homogeneity of characteristic values (temperature, flow-rate, composition...),
- Homogeneity of physical properties (density, viscosity...),
- Homogeneity of physical-chemical phenomena (mixing, reaction...),
- No variation of volume linked to the mixture of fluids (reactants).

The state and evolution of the homogeneous medium circulating inside a given cell k are then described by the following balance and constraint equations:

Global mass balance (mol.s⁻¹)

$$\frac{du_p^k}{dt} = F_p^{k-1} - F_p^k + \Delta n_p^k \times V_p^k \quad (1)$$

Component i mass balance (mol.s⁻¹)

$$\frac{d(u_p^k \times x_{p,i}^k)}{dt} = F_p^{k-1} x_{p,i}^{k-1} - F_p^k x_{p,i}^k + \Delta n_{p,i}^k \times V_p^k \quad (2)$$

Process energy balance (J.s⁻¹)

$$\begin{aligned} \frac{d(u_p^k \times H_p^k)}{dt} = & F_p^{k-1} H_p^{k-1} - F_p^k H_p^k + \Delta q_p^k \times V_p^k \\ & + h_{u_L}^k A_p^k (T_{u_L}^k - T_p^k) + h_{u_R}^k A_p^k (T_{u_R}^k - T_p^k) \end{aligned} \quad (3)$$

Pressure balance (Pa)

$$P_p^k = P_p^{k-1} - \Delta P_p^k \quad (4)$$

Volume constraint

$$F_p^k = 0 \quad (\text{during cell filling up}) \quad (5)$$

or

$$V_p^k = V_{cell}^k \quad (\text{once cell filling up achieved}) \quad (6)$$

3.2.2 Heat transfer modelling for normal operation

As shown in Figure 5, the following elements are involved in the heat balances described by the model:

- Reaction plate made of PEEK,
- Sandwich plates (SP1) (right and left),
- The area where the utility fluid flows (UF) (right and left),
- Sandwich plates (SP2) and transition plates (TP) association (called from now TP) (right and left).

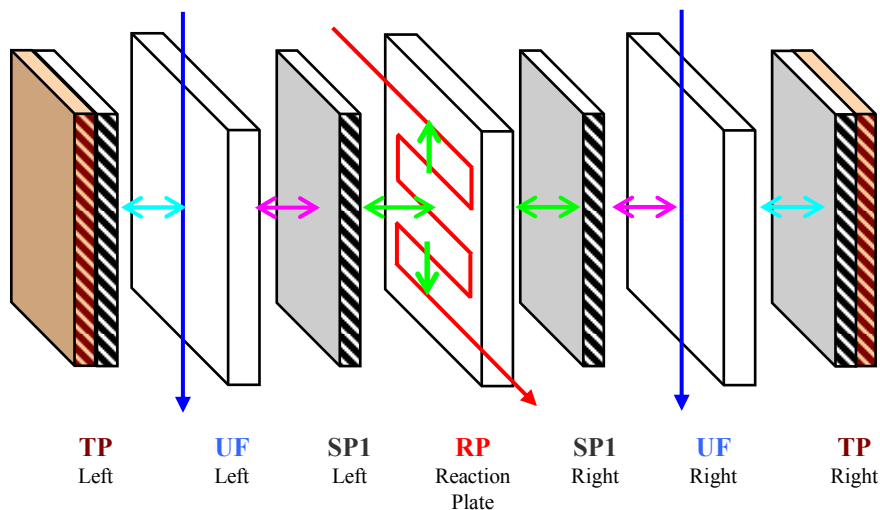


Figure 5. Heat transfer modelling in the inside structure of one block of the OPR

Heat transfer modelling leads to the following equations system (see Equations 7 to 10). As left and right sides involve the same equations, only equations related to left side are given.

Energy balance of the reaction plate made of PEEK (J.s^{-1})

$$\rho_{peek}^k V_{peek}^k C_{p_{peek}}^k \frac{dT_{peek}^k}{dt} = h_{p,peek}^k A^k (T_p^k - T_{peek}^k) \quad (7)$$

Energy balance of the left sandwich plate wall (J.s^{-1})

$$\rho_{sp_L}^k V_{sp_L}^k C_{p_{sp_L}}^k \frac{dT_{sp_L}^k}{dt} = h_{p,sp_L}^k A^k (T_p^k - T_{sp_L}^k) + h_{sp_L,u_L}^k A^k (T_{u_L}^k - T_{sp_L}^k) \quad (8)$$

Energy balance of the left utility fluid (J.s^{-1})

$$\rho_{u_L}^k V_{u_L}^k C_{p_{u_L}}^k \frac{dT_{u_L}^k}{dt} = F_{u_L}^k \rho_{u_L}^k C_{p_{u_L}}^k (T_{u_L}^{k-1} - T_{u_L}^k) + h_{sp_L,u_L}^k A^k (T_{sp_L}^k - T_{u_L}^k) + h_{u_L,tp_L}^k A^k (T_{tp_L}^k - T_{u_L}^k) \quad (9)$$

Energy balance of the left sandwich and transition plates (J.s^{-1})

$$\rho_{tp_L}^k V_{tp_L}^k C_{p_{tp_L}}^k \frac{dT_{tp_L}^k}{dt} = h_{u_L,tp_L}^k A^k (T_{u_L}^k - T_{tp_L}^k) \quad (10)$$

Each energy balance is associated with one or two local heat transfer coefficient:

- $h_{p,peek}^k$: local heat transfer coefficient between the process fluid and the reaction plate in PEEK,
- h_{p,sp_L}^k : local heat transfer coefficient between the process fluid and the sandwich plate on the left,
- h_{sp_L,u_L}^k : local heat transfer coefficient between the sandwich plate on the left and the utility fluid,
- h_{u_L,tp_L}^k : local heat transfer coefficient between the utility fluid and the transition plate on the left.

These coefficients, used in the energy balance equations, are necessary to evaluate the thermal phenomena taking place in the apparatus and to determine the evolution of temperature inside the process and utility fluids. They are calculated from two other parameters called film coefficients:

- h_p : process film coefficient,
- h_u : utility film coefficient.

Figure 6 allows one to see the location of these two coefficients during heat exchanges through the different plates of the OPR.

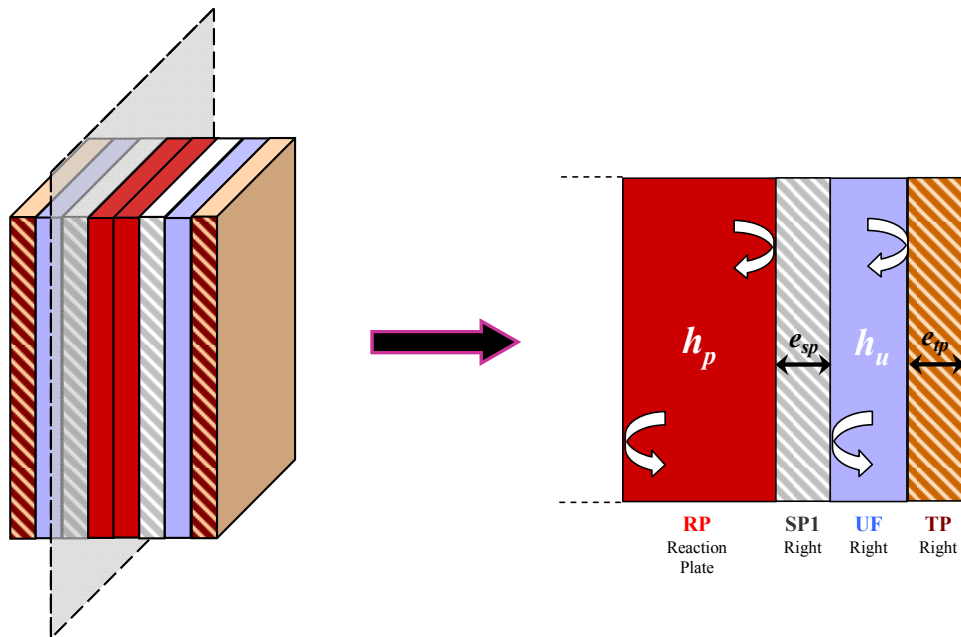


Figure 6. Localisation of the process and utility film fluid in one block of the OPR

The first coefficient, h_p , allows one to quantify the thermal exchanges taking place in the liquid film located at the interface between the process fluid and the sandwich plates (right and left). The latter, h_u , allows one to quantify the thermal exchanges taking place in the two liquid films located on one hand between the utility fluid and the sandwich plates (right and left) and on the other hand between the utility fluid and the transition plates (right and left). For each cell k , the local heat transfer coefficients are then estimated by the following equations:

Local heat transfer coefficient between the process fluid and the reaction plate in PEEK ($\text{W.m}^{-2}.\text{K}^{-1}$)

$$h_{p,peek}^k = \frac{l}{\frac{l}{h_p} + \frac{V_{peek}^k}{S_{peek}^k \cdot \lambda_{peek}}} \quad (11)$$

Local heat transfer coefficient between the process fluid and the sandwich plate on the left ($\text{W.m}^{-2}.\text{K}^{-1}$)

$$h_{p,sp_L}^k = \frac{l}{\frac{l}{h_p} + \frac{e_{sp}}{2 \cdot \lambda_{acier}}} \quad (12)$$

where e_{sp} is the sandwich plates thickness in mm.

Local heat transfer coefficient between the sandwich plate on the left and the utility fluid ($\text{W.m}^{-2}.\text{K}^{-1}$)

$$h_{sp_L,u_L}^k = \frac{l}{\frac{l}{h_u} + \frac{e_{sp}}{2 \cdot \lambda_{acier}}} \quad (13)$$

Local heat transfer coefficient between the utility fluid and the transition plate on the left ($\text{W.m}^{-2}.\text{K}^{-1}$)

$$h_{u_L,tp_L}^k = \frac{l}{\frac{l}{h_u} + \frac{V_{tp}^k}{S_{tp}^k \cdot \lambda_{acier}}} \quad (14)$$

During normal operation, when the fluids flow in the apparatus, the process and utility film coefficient are calculated considering a forced convection regime. Finally, the two following experimental correlations have been established:

Process film coefficient ($\text{W.m}^{-2}.\text{K}^{-1}$)

$$h_u = a \cdot F_u + b \quad (15)$$

Utility film coefficient ($\text{W.m}^{-2}.\text{K}^{-1}$)

$$h_p = (c \cdot Re^\alpha \cdot Pr^\beta \cdot \lambda_p) / (Dh) \quad (16)$$

where a , b , c , α , β are experimental constants, Re , Pr are Reynolds and Prandtl numbers, Dh is the hydraulic diameter and F_u the utility fluid.

4. APPLICATION CASE: OXIDATION OF SODIUM THIOSULFATE

4.1 Normal operation

When normally operated, the conditions of a typical oxidation experiment in the OPR are described in Table 2. The temperature recordings of the A, B, C, D, and E thermocouples, located along the reaction line in the first block, are available. On the other hand, the simulator can compute the temperature profile along the utility and reaction lines after the steady state has been established for a normal operation. Figure 7 represents the experimental and simulated results: temperature profiles of the utility and process fluids and molar conversion rate (X) with respect to $\text{Na}_2\text{S}_2\text{O}_3$ along the reaction line. It must be noticed that the utility fluid temperature slightly increases along the reaction line whereas the process fluid temperature goes through a maximum (about 30°C) in the middle of the first block and then becomes stabilized in the third block. We also notice that, at the reactor outlet, the conversion is not total (72 %). Besides, concerning the process fluid, this figure shows a good agreement with the measurements carried out with the thermocouples immersed in the reaction fluid and the simulation.

Table 2. Operating conditions of the thiosulfate oxidation reaction in the OPR

Utility fluid (glycol-water)		Feeding line 1 : sodium thiosulfate + water			Feeding line 2 : hydrogen peroxide + water		
Flowrate ($\text{m}^3.\text{h}^{-1}$)	T ($^\circ\text{C}$)	Flowrate (L.h^{-1})	T ($^\circ\text{C}$)	% weight of peroxide	Flowrate (L.h^{-1})	T ($^\circ\text{C}$)	% weight of peroxide
1.55	14.9	40.3	20	11.0	10.4	20	20.0

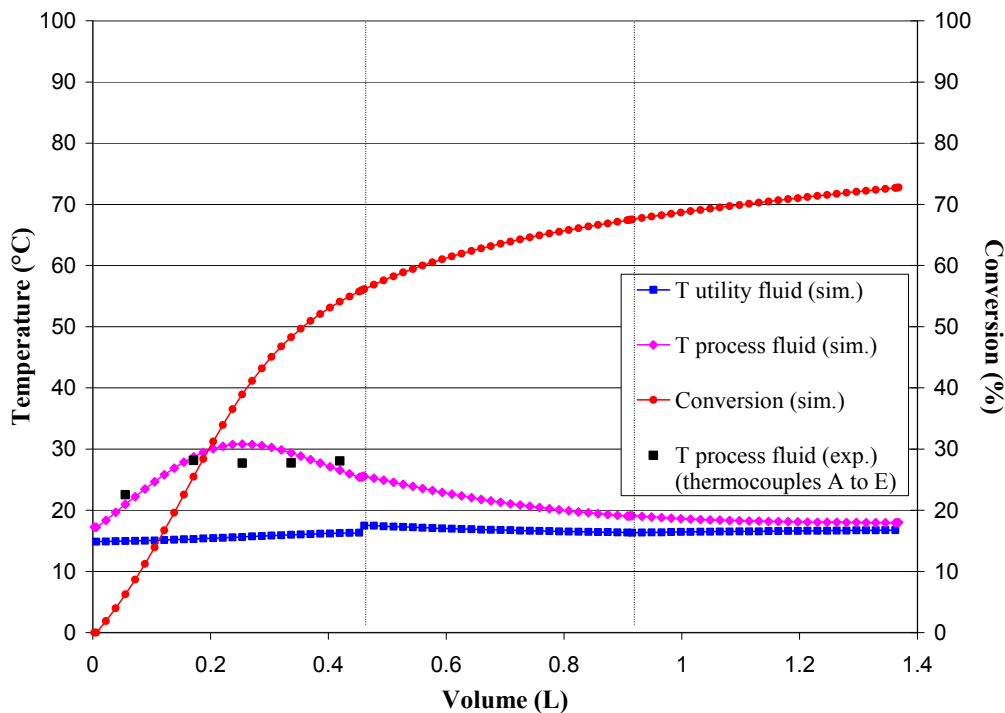


Figure 7. Temperature and conversion profiles of the oxidation reaction in the OPR when normally operated

4.2 Failure mode: experimental results

After establishing the permanent normal operating conditions, a cooling failure is caused by stopping the “utility” fluid flow. Figure 8 represents the variations of the process fluid temperature in the first block (A to E thermocouples) and utility fluid flowrate as a function of time.

Three important phases are noted:

- Phase 1 (4100 s to 4235 s): the reaction mixture temperature is stable. A steady state is reached.
- Phase 2 (4235 to 4320 s): the utility fluid flowrate is nil. An increase of the reaction mixture temperature is observed, due to the absence of cooling.
- Phase 3 (from 4320 s on): the utility fluid flowrate is brought back to its initial value. The reaction mixture temperature decreases again to reach a steady state.

According to the operating conditions of the oxidation reaction detailed in Table 2, the adiabatic temperature rise, ΔT_{ad} , is 85 °C. Figure 8 shows a maximum temperature rise of about 40 °C (Th B) between the two phases 2 and 3. The utility fluid flowrate, which is 30 times larger than the process fluid flowrate,

is able to make the process temperature decrease at the precise time it is brought back to $1.5 \text{ m}^3 \cdot \text{h}^{-1}$. Without this action on the utility flowrate, the temperature of the process fluid could have reached more than 110°C and cause an over pressure in the reaction plates.

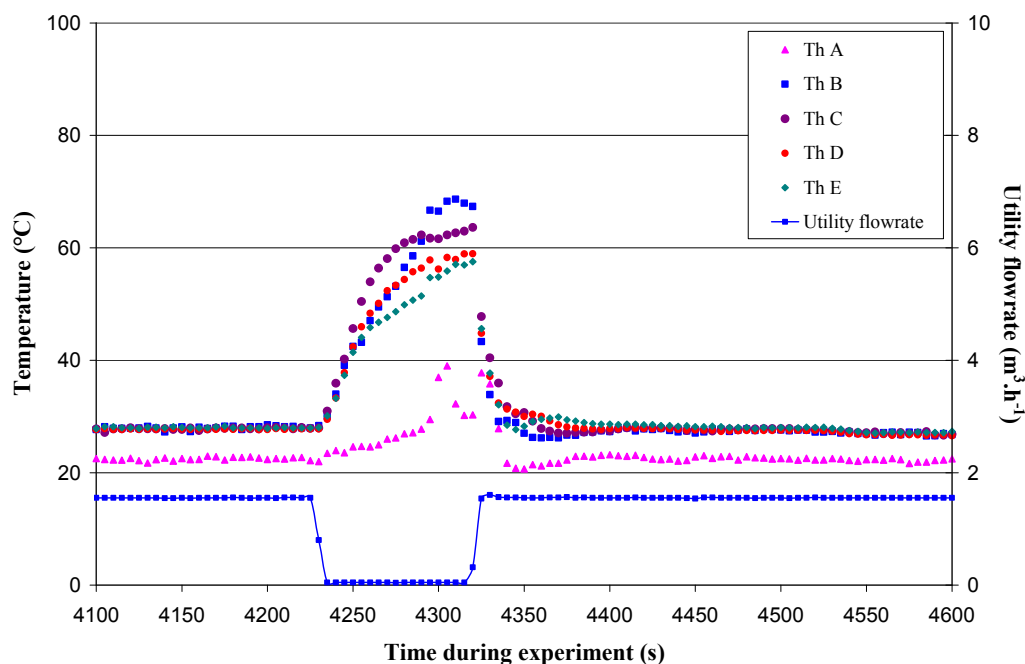


Figure 8. Temperature experimental profiles of the reaction mixture and utility fluid flowrate as a function of time in the OPR

4.3 Failure mode: evaluation of the heat transfer mode

As explained in chapter 3.2.2, the average coefficient of heat transfer between the “utility” fluid and the “sandwich” plates, which delimit the flow zone, is the film heat transfer coefficient h_u . The value of this coefficient depends on the heat transfer mode. During normal operation, this coefficient is calculated with correlations established in a forced convection mode. According to Equation 15, it is equal to $36000 \text{ W} \cdot \text{m}^{-2} \cdot \text{K}^{-1}$ for a utility fluid flowrate of $1.55 \text{ m}^3 \cdot \text{h}^{-1}$. The stoppage of the utility fluid flowrate involves a change in the heat transfer mode. Three hypothesis are possible:

- Pure conduction,
- Natural free convection,
- Both phenomena at the same time.

Let us first consider that heat transfer is only due to conduction. h_u can then be evaluated by the following equation:

$$h_u = \frac{2 \cdot \lambda_u}{e_{UF}} = 200 \text{ W.m}^{-2}.\text{K}^{-1} \quad (17)$$

where e_{UF} is the thickness of the utility fluid flow zone and λ_u the thermal conductivity of this fluid (glycol-water mixture).

The computer model is used to simulate the consequences of a variation of an operating condition at a time fixed by the user on the OPR dynamic behaviour. In particular, if the flowrate of the “utility” fluid becomes nil, we consider that there is no mass exchange between cells on the “utility” fluid side and the value of heat transfer coefficient can be modified because the heat transfer mode is no longer linked to forced convection.

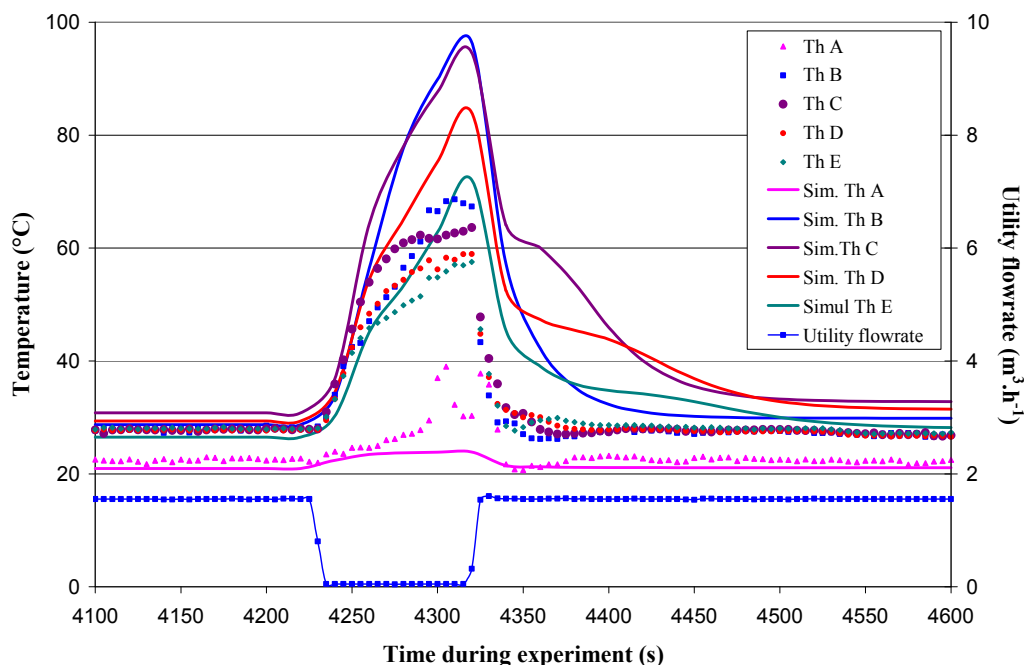


Figure 9. Experimental and simulated temperature profiles of the reaction mixture as a function of time in the OPR: hypothesis of the conductive heat transfer mode during a “utility” fluid stop: $h_u = 200 \text{ W.m}^{-2}.\text{K}^{-1}$.

Figure 9 provides a comparison between the temperature profiles of the reaction mixture measured and simulated when the coefficient h_u , included in the model, goes from a value of $36000 \text{ W.m}^{-2}.\text{K}^{-1}$ to the value of $200 \text{ W.m}^{-2}.\text{K}^{-1}$. We observe that profiles are in agreement in the first moments that follow the utility fluid stoppage. Hereafter, the temperatures obtained by simulation are much higher (about 30°C) than the measured values. These differences lead us to think

that heat transfer involves more than conduction alone. It is possible that some of the heat transfer is given by natural convection.

We thus propose to evaluate the value of h_u when the heat transfer mode is only due to natural convection. By assuming that each utility plate model cell is a closed rectangular cavity 3.3 mm (δ) thick and 18 mm (H) high limited by the vertical planes of two sandwich plates, we can then consider that natural free convection is produced in a liquid volume with the same dimensions. According to Incropera et al. (1981), the average heat transfer coefficient by natural free convection, h_u , existing within a fluid in a rectangular vertical closed cavity can be evaluated by the following equation:

$$Nu_{\delta} = 0.42 (Gr Pr)^{0.25} Pr^{0.012} \left(\frac{H}{\delta} \right)^{-0.3} = \frac{h_u \delta}{\lambda_u} \quad (18)$$

with $10 < H / \delta < 40$; $1 < Pr < 2.10^4$; $10^4 < GrPr < 10^7$

For our case study, we calculate:

$$Gr = 21000$$

$$Pr = 131$$

$$Gr.Pr = 2.74.10^6$$

$$H / \delta = 5.45$$

The result for H / δ outside the limits defined but really closed of the inferior limit. We considered that these values are acceptable.

Taking into account the corresponding experimental data, we obtain for the film coefficient:

$$h_u = 1200 \text{ W.m}^{-2}.\text{K}^{-1}$$

Figure 10 shows a comparison between the experimental and simulated temperature profiles of the reaction mixture when the coefficient h_u is equal to $200 \text{ W.m}^{-2}.\text{K}^{-1}$ during the first 20 seconds (time compatible with the heat transfer properties of PEEK), then to $1200 \text{ W.m}^{-2}.\text{K}^{-1}$ till starting up again the utility fluid.

We did not obtain an exact superposition of the two types of curves, especially when the utility fluid is stated up again: the experimental curves decrease faster than the simulated ones. However, we note a better representation of the experimental data which seems to confirm the hypothesis adopted previously.

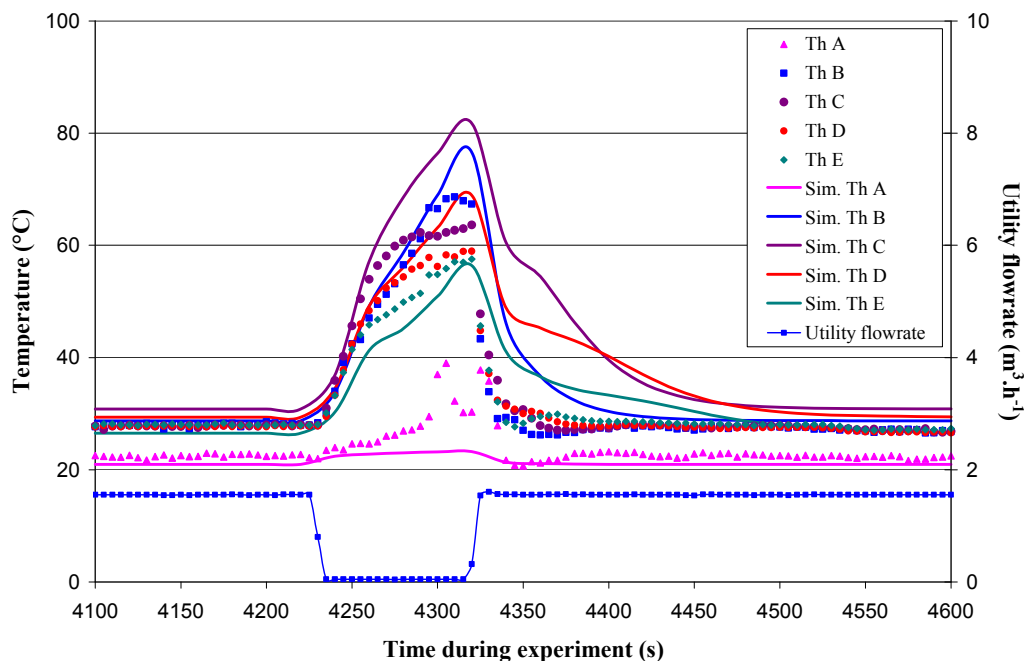


Figure 10. Experimental and simulated temperature profiles of the reaction mixture as a function of time in the OPR: heat transfer mode by conduction ($h_{fu} = 200 \text{ W m}^{-2} \text{ K}^{-1}$) then by natural convection ($h_{fu} = 1200 \text{ W m}^{-2} \text{ K}^{-1}$).

5. CONCLUSION

This work is part of a more general study dealing with the safety of intensified continuous reactors (Benaïssa et al., 2007). We studied the dynamical behaviour of a “heat-exchanger/reactor” in the case of a functional deviation corresponding to a “utility” fluid stoppage, identified in a HAZOP analysis of the OPR (Benaïssa et al., 2006) as the worst accidental scenario.

The first goal of this study was to check if the simulation tool, developed for normal operation, could be used to reproduce the failure mode. The first results are encouraging: even if the two types of curves don't agree perfectly, they have the same evolution over time. One condition is that the heat transfer film coefficient has to be changed in the model as a function of time according to the heat transfer modes taking place in the OPR. This first experimental approach showed that a heat transfer by natural convection should be added to the conduction after the utility fluid flow stoppage. As a perspective, more theoretical thermal studies have to be done to adjust more precisely the value and evolution of this coefficient which is a function of the type of apparatus taking into account hydrodynamics, material, geometry,... Indeed, this work also showed that the

“heat-exchanger/reactor” structure can influence the process temperature evolution: by conduction, natural free convection or both, an important part of the heat released by the reaction could be dissipated in the different plates (utility fluid zone is assumed to be a solid after the flow stoppage). The maximum temperature reached in the reaction medium will then be inferior to that evaluated when taking into account the adiabatic temperature rise, hypothesis commonly adopted to describe thermal runaway scenarios in batch reactors (Stoessel, 1993). This thermal behaviour confers an additional characteristic to the “heat-exchanger/reactor” which contributes to making it an intrinsically safer device.

To confirm this hypothesis and improve the modelling of the thermal behaviour of the OPR after a failure, other thermal runaway experiments should be done. Nevertheless, in regards to the potential risks, this kind of experiment has to be carried out in a appropriate environment and with a specific operating device in order to avoid any accident.

NOTATION

a	parameter in Equation (15)
A	exchange surface area, m^2
b	parameter in Equation (15)
C_p	heat capacity, $\text{J.kg}^{-1}.\text{K}^{-1}$
D_h	hydraulic diameter, m
F	flowrate, $\text{m}^3.\text{h}^{-1}$
h	local heat transfer coefficient, $\text{W.m}^{-2}.\text{K}^{-1}$
H	enthalpy, J.mol^{-1}
h_p	process film coefficient, $\text{W.m}^{-2}.\text{K}^{-1}$
h_u	utility film coefficient, $\text{W.m}^{-2}.\text{K}^{-1}$
P	pressure, bar
t	time, s
T	temperature, $^{\circ}\text{C}$
V	volume, m^3
S	surface, m^2
x	molar fraction, %
X	molar conversion, %

Abbreviation

Gr	Grashof number
OPR	Open Plate Reactor
PEEK	polyetheretherketone
Pr	Prandtl number
Th	thermocouple

TP	transition plate
Re	Reynolds number
RP	reaction plate
SP	sandwich plate
UF	utility fluid

Greek Letters

α	parameter in Equation (16)
β	parameter in Equation (16)
λ	thermal conductivity, $\text{W.m}^{-1}.\text{K}^{-1}$
ρ	mass volume, kg.m^{-3}
Δn	global molar production rate of the reaction, $\text{mol.m}^{-3}.\text{s}^{-1}$
Δq	heat released by the reaction, $\text{J.m}^{-3}.\text{s}^{-1}$
ΔT_{ad}	adiabatic temperature rise, $^{\circ}\text{C}$

Subscripts

i	component
k	number of a modelled cell
L	left
p	process
R	right
u	utility

REFERENCES

- Benaïssa, W., Elgue, S., Gabas, N., Cabassud, M., Carson, D., “Transposition of an exothermic reaction to a continuous intensified reactor”, Sustainable (Bio)Chemical Process Technology, 2005, Jansens/Stankiewicz/Green, 69-77.
- Benaïssa, W., Elgue, S., Gabas, N., Cabassud, M., Carson, D., “Hazard Identification and Risk Assessment in an Intensified Heat Exchanger/reactor”, CISAP-2, Chemical Engineering Transactions, 2006, 9:133-138
- Benaïssa, W., “Développement d’une méthodologie pour la conduite en sécurité d’un réacteur continu intensifié”, 2006, PhD thesis, Institut National Polytechnique from Toulouse (INP).
- Benaïssa, W., Gabas, N., Cabassud, M., Demissy, M., Carson, D., “Safety methodology for the operation of a continuous intensified reactor”, IChemE Symposium N°153, Edinburgh, 2007.

Cohen, W.C., Spencer, J.L., "Determination of Chemical Kinetics by Calorimetry", Chemical Engineering Progress, 1962, Vol. 58, 12, 40-41.

Elgue, S., Devatine, A., Prat, L., Cognet, P., Cabassud, M., Gourdon, C., Chopard, F., "Dynamic Simulation of a Novel Intensified Reactor", ESCAPE 14, LISBONNE Portugal 2004.

Elgue, S., Chopard, F., Cabassud, M., Cognet, P., Prat, L., Gourdon, C., "Optimisation d'une Réaction Chimique dans un Réacteur Ouvert du type à plaque", Patent FR 0500424, 24th january 2005.

Elgue, S., Devatine, A., Prat, L., Cognet, P., Cabassud, M., Gourdon, C., Chopard, F., "Dynamic simulation of a novel intensified reactor", Computer and Chemical Engineering, submitted, 2008.

Incropera, F.P., Dewitt, D.P., "Fundamentals of Heat Transfer", 1981, John Wiley and Sons, New York.

Lin, K.F., Wu, J.L., "Performance of an Adiabatic Controlled Cycled Stirred Tank Reactor", Chemical Engineering Science, 1981, 36, 435-444.

Lo, S.N., Cholette, A., "Experimental Study on the Optimum Performance of an Adiabatic MT Reactor", The Canadian Journal of Chemical Engineering, 1972, Vol. 50, 71-80.

Neuman, E.B., "Chemical reactor design, optimization, and scaleup", 2002, McGraw-Hill,

Prat, L., Devatine, A., Cognet, P., Cabassud, M., Gourdon, C., Elgue, S., Chopard, F., "Performance Evaluation of a Novel Concept Open Plate Reactor Applied to Highly Exothermic Reaction", Chemical Engineering Technology, 2005, 28(9), 1028-1034.

Stoessel, F., "What is your thermal risk?", Chemical Engineering Progress, 1993, October, 68-75.